

## First-principles study of field emission of carbon nanotubes

Seungwu Han<sup>1,2</sup> and Jisoon Ihm<sup>1,\*</sup>

<sup>1</sup>*School of Physics, Seoul National University, Seoul 151-742, Korea*

<sup>2</sup>*Princeton Materials Institute, Princeton University, Princeton, New Jersey 08544*

(Received 17 October 2002; published 13 December 2002)

Field emission properties of the (10,10) carbon nanotube are investigated with a first-principles approach. Emission currents are obtained through integrations of the time-dependent Schrödinger equation. We find that the emission current from the states localized at the tip end is more than ten times greater than direct contributions from extended metallic ( $\pi$  and  $\pi^*$ ) states. The spatial distribution of the electronic wave function as it tunnels through the energy barrier is shown in time sequence. The simulated image on the screen shows a pentagonal pattern in agreement with experiment.

DOI: 10.1103/PhysRevB.66.241402

PACS number(s): 79.70.+q, 71.15.Dx, 73.63.Fg

Carbon nanotubes have been regarded as a promising material to be used as electron emitters in the field emission display (FED).<sup>1</sup> The unusually high aspect ratio as well as the mechanical and chemical stability of the nanotube are main advantages over the conventional metallic tips. The viability toward the practical device application is being examined, and the carbon-nanotube-based FED is expected to be commercialized in the near future.<sup>2</sup>

To improve the performance of the nanotube field emitter by tuning the structural parameters such as the radius, end geometry, and packing density, it is essential to understand the emission mechanism of the nanotube. While the Fowler-Nordheim (F-N) theory<sup>3</sup> has been successful in describing the field emission of micron-sized tips, many experiments reflect that the F-N theory is not sufficient for a full understanding of the field emission of nanotubes. Examples are nonlinear I-V characteristics in the F-N plots<sup>4</sup> and the photoluminescence during field emission with a pronounced peak at a certain frequency.<sup>5</sup> In addition, the energy distribution of emitted electrons exhibits a sharp peak which shifts to a lower energy side almost linearly as the applied field increases.<sup>6</sup> All of these observations are incompatible with the picture that the emission current originates purely from the usual metallic (extended) states, suggesting that localized states<sup>7</sup> may contribute to the emission current significantly.

On the theory side, one is faced with many difficulties when trying to make a quantitative prediction on the field emission of nanotubes; since the applied voltage is usually very high (a few hundred to a few thousand volts) and the local field at the tip of the nanotube is extremely large ( $\sim 1$  V/Å), the linear response evaluation of the emission current is not justified. Furthermore, the localized electronic states at the tip of the nanotube, which are not taken into account in the F-N-type simplified model, may profoundly affect the emission. The usual scattering formalism<sup>8</sup> is not adequate for describing the field emission of the localized states since they are not current-carrying states.

Recently, we proposed an *ab initio* method for computing field emission currents of nanostructures.<sup>9</sup> In short, this method starts with performing first-principles calculations on the nanotip under the electric field, thereby obtaining the self-consistent potential and the wave functions. To confine the electronic charge within the emission tip during the self-

consistency cycle, either a large barrier is applied temporarily outside the tip or a localized basis set is employed. With the computed eigenstates as initial electronic configurations, the temporal wave functions are determined by solving the time-dependent Schrödinger equation. The transition rate (the amount of charge flowing out of the tip per unit time) is then evaluated, and the total current is obtained by summing up the product between the transition rate and the occupation number of individual states. This method has been applied to the field emission of carbon chains<sup>9</sup> and graphitic ribbons.<sup>10</sup>

In this article, we use the above method to elucidate a detailed emission mechanism of the single-wall carbon nanotube. As a model system, we take a (10,10) carbon nanotube with a symmetric cap at the end. Its diameter of 1.4 nm corresponds to a typical size of single-wall nanotubes used in the field-emission experiments.<sup>2</sup> The length of the nanotube is chosen to be 40 Å containing 630 carbon atoms. The size of the supercell in the periodic boundary condition is 45 Å  $\times$  45 Å  $\times$  75 Å, large enough to avoid the interaction between repeated systems.

First, we analyze the electronic structure of the nanotube under applied electric fields ( $E_{\text{appl}}$ ), employing the standard *ab initio* pseudopotential method<sup>11</sup> with the local density approximation.<sup>12</sup> In expanding the wave function, we use the localized orbitals of the minimal  $sp^3$  type.<sup>13</sup> This basis set accurately describes the structural and electronic properties of the carbon system with relatively small distortions with respect to the graphite, such as the nanotube or fullerene.<sup>14</sup> The plane waves with the cutoff energy of 40 Ry are used in representing the potential. The uniform external electric field is simulated as a sawtooth-type potential to be compatible with the periodic boundary condition. The magnitude of the external field is chosen so that the local electric field at the tip of the model nanotube is about the same as the value in experimental situations. An empirical rule that the local electric field is essentially a function of the product between the tube length and the external electric field turns out to be useful here.<sup>15</sup> The atomic coordinates are relaxed at zero external field.<sup>16</sup> In Fig. 1, the electronic distributions are plotted along the nanotube for  $\pi$ ,  $\pi^*$ , and localized states close to the Fermi level, showing that the localized state decays fast

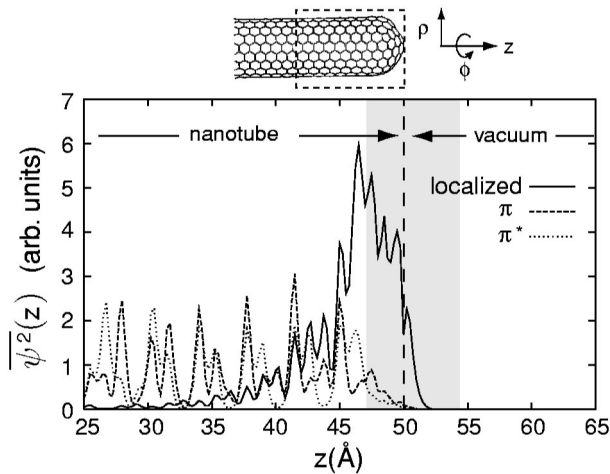


FIG. 1. The electronic distribution along the nanotube for extended ( $\pi$  and  $\pi^*$ ) and localized states close to the Fermi level. The squared wave functions are averaged over  $\rho$  and  $\phi$ . The model on the top shows the nanotube region plotted. The shaded region is where the local electric field is larger than  $1.5 \text{ V/\AA}$  when  $E_{\text{appl}}$  is  $0.7 \text{ V/\AA}$  (see text).

away from the cap while the distribution of the extended states is rather uniform over the tube body.

As we increase  $E_{\text{appl}}$  from zero, noticeable changes are observed in the occupation number and the energy level of the localized states (see Fig. 2). At low fields, doubly degenerate localized states exist above the Fermi level which do not contribute to the current because they are unoccupied. When  $E_{\text{appl}}$  exceeds  $0.2 \text{ V/\AA}$ , the occupation number (or filling factor)  $f$  is linearly increased until it reaches 1. To explain the linear filling of the localized states, we examine each component of the total energy as the localized state is filled. It is found that the filling factor of the localized states is determined mainly by the balance of two terms—the external potential term and the electron-electron repulsion term induced by the accumulation of charge in the cap. This observation enables us to explain the intermediate re-

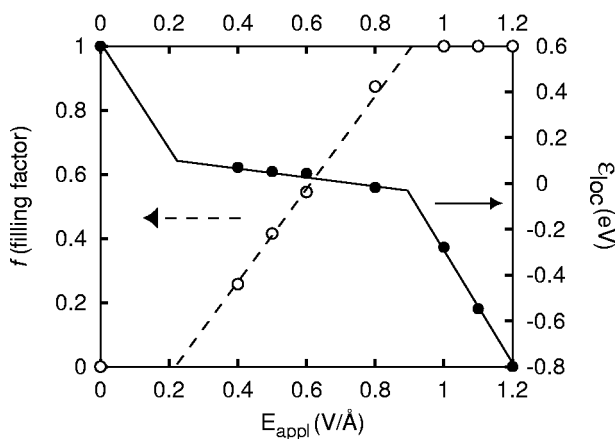


FIG. 2. Filling factor  $f$  (open circles) and energy level of localized states  $\epsilon_{\text{loc}}$  with respect to the Fermi level (filled circles) as a function of the external field ( $E_{\text{appl}}$ ). The solid and dashed lines are guides to the eye.

gion of Fig. 2 in terms of energy minimization; the total energy change  $\Delta U$ , by adding a charge  $-4ef$  (4 is the number of localized states including the spin degeneracy and  $-e$  is the electron charge) for a given  $E_{\text{appl}}$  can be approximated as

$$\Delta U(f) = -4ef\alpha E_{\text{appl}} + \frac{(\rho_{\text{cap}} - 4ef)^2 - \rho_{\text{cap}}^2}{2C_{\text{cap}}}, \quad (1)$$

where  $\alpha E_{\text{appl}}$  is the effective electric potential shift experienced by the localized state with respect to the potential deep inside the tube. This term reflects the fact that the potential shift is proportional to  $E_{\text{appl}}$ . The second term is the Coulomb energy contributed by the extra charge ( $-4ef$ ) added to the original electronic charge in the cap ( $\rho_{\text{cap}}$ ).  $C_{\text{cap}}$  is the capacitance of the cap which is related to its size and geometry. Minimizing  $\Delta U$  with respect to  $f$ , we have

$$f = \alpha E_{\text{appl}} \frac{C_{\text{cap}}}{4e} + \frac{\rho_{\text{cap}}}{4e}, \quad (2)$$

showing that  $f$  is linear in  $E_{\text{appl}}$ . In the case of the (5,5) nanotube, we find that the increase of  $f$  is again linear in  $E_{\text{appl}}$  but slower than in Fig. 2. This is consistent with Eq. (2) since the smaller size of the cap leads to a smaller  $C_{\text{cap}}$ .

While  $f$  increases from 0 to 1, the Fermi level is more or less pinned by these localized states. Once  $f$  reaches 1, the energy level of the localized states shifts down much more rapidly by a further increase in the applied bias because the screening is now less complete. As will be shown below, the localized states are the main source of the emission current, and this region ( $f=1$ ) corresponds to the experimental situation where the peaks in the energy spectrum shift significantly as a linear function of the external field.<sup>6</sup> Continuum metallic states originating from the body of the nanotube do not undergo such a shift since its peak is fixed at the Fermi level. We note that the localized states in Fig. 2 are orthogonal to the continuum states at the same energy level due to the symmetry incompatibility; under the operation of the  $2\pi/5$  rotation in the  $\phi$ -direction (see Fig. 1), the eigenvalue (i.e., the phase factor) of the localized state is  $e^{i2/5\pi}$  while those for the extended  $\pi$  and  $\pi^*$  states are 1.

To obtain the emission current, we integrate time-dependent Schrödinger equations with the split-operator method.<sup>17</sup> The basis set for expanding the wave function is switched to plane waves to describe the tunneling process of electrons. The simulation time of 1.5 fs is appropriate to evaluate the transition rate from the slope of the electron leakage curve. If the simulation time were too long, the front of the wave function of the emitted electron would reach the boundary of the supercell and be reflected, causing undesirable oscillations in the amplitude. Figure 3 shows the emission current of  $\pi$ ,  $\pi^*$ , and localized states. It is noticeable that the contribution from localized states dominates ( $\sim 95\%$  of the total current) over the whole range of  $E_{\text{appl}}$  studied. The large currents of localized states were also observed in the (5,5) nanotube.<sup>9</sup> The pronounced contribution of localized states can be understood from the electronic distributions presented in Fig. 1. The localized states are ex-

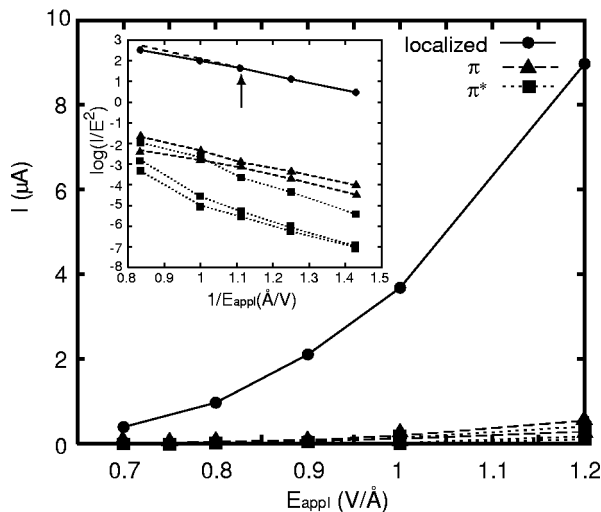


FIG. 3. The emission current of each state as a function of the external electric field. The inset shows the F-N plot. The dashed line and the arrow are drawn in the inset to emphasize the change of the slope for the localized state.

posed to the high field region (shaded box in Fig. 1) with substantially larger amplitudes than extended states, implying that the average tunneling distance for the localized state is smaller than that for extended states. This leads to a large variation of the current between localized and extended states as the emission current depends on the tunneling distance exponentially.

The F-N plots in the inset of Fig. 3 show almost straight lines as predicted by the F-N theory. The slope in the F-N plot for the localized state changes slightly at the point indicated by an arrow. The abrupt change of  $df/dE_{\text{appl}}$  near  $f=1$  mentioned above leads to this change since the emission current is the product of  $f$  and the transition rate. This may partially account for the experimental observation of the nonlinear F-N plots.<sup>4</sup> However, it is noted that the actual change of the slope in experiment is several times greater than what is found here and other causes such as the adsorption of ambient molecules should play a major role.<sup>18</sup>

It is also interesting in Fig. 3 that the current of the  $\pi$  state is 2–3 times greater than that of the  $\pi^*$  state. Due to a rotational symmetry of the (10,10)-capped nanotube around its axis, each state in the nanotube tunnels to vacuum states with the same symmetry component. The constant phase of the  $\pi$  state around the circumference of the nanotube enables the  $\pi$  state to couple with the vacuum state with zero angular momentum in the cylindrical coordinate of the nanotube ( $m_\phi=0$ ; see Fig. 1). However, the phase of the  $\pi^*$  state changes much more rapidly and the corresponding vacuum state also has a larger angular momentum component ( $m_\phi=10$ ). This leads to a smaller tunneling integral between them and hence smaller emission currents.

As an example of a different end geometry, we have also studied the open (10,10) nanotube with hydrogen passivation at the end. In this case, there is no localized state within the relevant energy range. However, the extended states are now

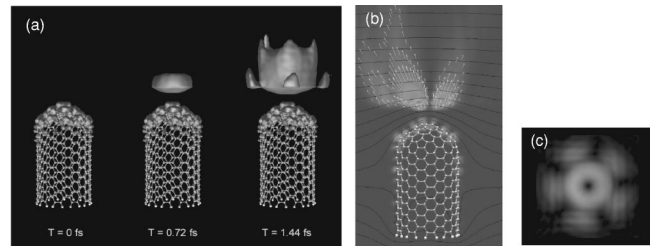


FIG. 4. (a) Snapshots of the charge distribution of emitted electrons (doubly degenerate localized states) from the capped (10,10) nanotube. The amplitude of the wave function is magnified by 30 times in the vacuum region for the visual purpose. (b) The current density of one of the localized states at the last instance of (a). The electronic density and the equipotential lines are also displayed. (c) The simulated image on the screen.

touching the high field region with much larger amplitudes than in the capped nanotube, thus greatly facilitating the field emission. This, in combination with the ability to couple with the  $s$ -like vacuum state, significantly enhances the emission current of the  $\pi$  state almost to the level of the localized states of the capped nanotube.

Figure 4(a) illustrates an example of the temporal sequence of the electronic configuration under the external electric field. It captures instantaneous configurations of the doubly degenerate localized states flowing out of the tunneling barrier and exhibits a characteristic charge density distribution in space. In Fig. 4(b), the current densities (indicated by arrows) are shown for one of the localized states at  $t = 1.44$  fs, drawn on a plane lying on the nanotube axis. The equipotential lines show that the electron is driven along the gradient of the potential.

One can also simulate the microscopic image on the phosphor screen of the FED by plotting the amplitudes of the wave function on a plane in front of the nanotube. Figure 4(c) is such a simulated image on the screen contributed from doubly degenerate localized states. The image of a ring surrounded by five spots is similar to the one observed in a recent experiment of the field-emission microscopy of carbon nanotubes.<sup>19</sup> For the open (10,10) nanotube (not shown), we find that the extended  $\pi$  states produce a single spot because of the large amplitude of the  $s$ -like vacuum state.

For the localized electrons to be emitted to the anode side persistently, electrons must be supplied from the extended states forming the current loop (circuit). The coupling between the extended states and the localized states estimated from experimental broadening of the localized states is 0.1 eV, which corresponds to the transition rate of  $10^{14}/\text{s}$ .<sup>6</sup> On the other hand, the emission rates of localized states across the barrier are  $10^{11}/\text{s}$  and  $10^{12}/\text{s}$ , respectively, when the local fields at the tip are  $\sim 1$  V/Å and  $\sim 1.5$  V/Å. Since this process is much slower than the intratube transition rate of  $10^{14}/\text{s}$ , the rate-limiting step of the whole process is the tunneling of the localized states into the vacuum. It also implies that the joule heating would occur at the edge of the nanotube. The potential drop within the nanotube near the edge is  $\sim 0.1$  V from the calculated self-consistent potential. When

the local field at the tip is  $\sim 1 \text{ V/\AA}$ , the current of a single-wall nanotube is  $\sim 10 \text{ nA}$  (a typical value to produce enough brightness on the screen when an array of nanotube emitters exists in the FED device) and the joule heating per tube is  $\sim nW$ , which is small enough not to raise the temperature significantly.

We thank Prof. R. Car for helpful discussions. This work is supported by the CNNC of the Sungkyunkwan University. SH's work at Princeton University is supported by KOSEF. The computations were supported by the Grand Challenge Program of the Supercomputing Center of KISTI.

\*Author to whom correspondence should be addressed. Email: jihm@snu.ac.kr

<sup>1</sup>P.G. Collins and A. Zettl, *Appl. Phys. Lett.* **69**, 1969 (1996); J.-M. Bonard *et al.*, *ibid.* **73**, 918 (1998).

<sup>2</sup>W.B. Choi *et al.*, *Appl. Phys. Lett.* **75**, 3129 (1999); N.S. Lee *et al.*, *Jpn. J. Appl. Phys., Part 1* **39**, 7154 (2000).

<sup>3</sup>R.H. Fowler and L. Nordheim, *Proc. R. Soc. London, Ser. A* **119**, 173 (1928).

<sup>4</sup>P.G. Collins and A. Zettl, *Phys. Rev. B* **55**, 9391 (1997); S. Dimitrijevic *et al.*, *Appl. Phys. Lett.* **75**, 2680 (1999); X. Xu and G.R. Brandes, *Appl. Phys. Lett.* **74**, 2549 (1999).

<sup>5</sup>J.-M. Bonard *et al.*, *Phys. Rev. Lett.* **81**, 1441 (1998).

<sup>6</sup>M.J. Fransen, Th.L. van Rooy, and P. Kruit, *Appl. Surf. Sci.* **146**, 312 (1999).

<sup>7</sup>R. Tamura and M. Tsukada, *Phys. Rev. B* **52**, 6015 (1995); P. Kim *et al.*, *Phys. Rev. Lett.* **82**, 1225 (1999).

<sup>8</sup>Ch. Adessi and M. Devel, *Phys. Rev. B* **62**, R13314 (2000).

<sup>9</sup>S. Han, M.H. Lee, and J. Ihm, *Phys. Rev. B* **65**, 085405 (2002); S. Han, M.H. Lee, and J. Ihm, *J. Korean Phys. Soc.* **39**, 564 (2001).

<sup>10</sup>K. Tada and K. Watanabe, *Phys. Rev. Lett.* **88**, 127601 (2002).

<sup>11</sup>N. Troullier and J.L. Martins, *Phys. Rev. B* **43**, 1993 (1991).

<sup>12</sup>W. Kohn and L.J. Sham, *Phys. Rev.* **140**, A1133 (1965).

<sup>13</sup>O.F. Sankey and D.J. Niklewski, *Phys. Rev. B* **40**, 3979 (1989).

<sup>14</sup>G.B. Adams *et al.*, *Phys. Rev. B* **44**, 4052 (1991); N. Park *et al.*, *Phys. Rev. B* **65**, 121405 (2002).

<sup>15</sup>S. Han and J. Ihm, *Phys. Rev. B* **61**, 9986 (2000).

<sup>16</sup>Supplementary calculations on the (5,5) nanotube indicate that the C-C bonding changes less than  $0.05 \text{ \AA}$  even at the largest field ( $1.2 \text{ V/\AA}$ ).

<sup>17</sup>M. Suzuki, *Phys. Lett. A* **146**, 319 (1990); O. Sugino and Y. Miyamoto, *Phys. Rev. B* **59**, 2579 (1999).

<sup>18</sup>K.A. Dean and B.R. Chalamala, *Appl. Phys. Lett.* **76**, 375 (2000).

<sup>19</sup>Y. Saito, K. Hata, and T. Murata, *Jpn. J. Appl. Phys.* **39**, L271 (2000).